Int. J. Environ. Sci. Technol. (2016) 13:825–834
DOI 10.1007/s13762-015-0920-0

ORIGINAL PAPER

Development of attapulgite composite ceramsite/quartz sand double-layer biofilter for micropolluted drinking source water purification

Z. Wang[1,2] · M. G. Zhong[1] · J. F. Wan[2,3,4] · G. J. Xu[2] · Y. Liu[2,3]

Received: 23 April 2015 / Revised: 7 November 2015 / Accepted: 13 December 2015 / Published online: 7 January 2016

Abstract This study compared start-up and steady-state affecting factors of attapulgite composite ceramsite/quartz sand double-layer biofilter (ACC/QSDLBF) and quartz sand single-layer biofilter (QSSLBF) on micropolluted drinking source water treatment. Results showed that the ACC has suitable pore size distribution in the range of 5–850 nm which is conducive to biofiltration. Turbidity removal efficiency of ACC/QSDLBF was a little lower than QSSLBF, but organic matters and ammonia removal efficiencies of ACC/QSDLBF were much higher than QSSLBF due to biodegradation and nitrification by microorganisms colonizing on the ACC. At stable state, the growth of head loss for ACC/QSDLBF was lower than that of QSSLBF. The complete filtration cycle of ACC/QSDLBF was 52 h. The total COD_{Mn} removal rate of ACC/QSDLBF was 20.93 %, in which 90 % of removed total COD_{Mn} was achieved at the upper 60 cm of ACC filter layer. The removal of COD_{Mn} decreased from 35.89 to 13.16 % in ACC/QSDLBF when increasing hydraulic loading from 2 to 16 m/h. After analysis of efficient EBCT in ACC/QSDLBF, optimized hydraulic loading was 12 m/h. These conclusions would be helpful to practical application of ACC as functional material for new construction of waterworks, especially upgrading of existing waterworks treating micropolluted drinking source water.

Keywords Attapulgite composite ceramsite · ACC/QSDLBF · Biofiltration · Start-up · Affecting factors · Efficient EBCT (EEBCT)

Introduction

In developing countries, large quantities of wastewater without proper treatment have been discharged into various water bodies, leading to serious deterioration of surface water quality (Zhang et al. 2014). Organic matters and ammonia have been identified as major pollutants in source water and can cause water eutrophication and problems associated with drinking water disinfection by-products (Xiang et al. 2013; Zhang et al. 2013a, b; Li et al. 2014). It had been reported that more than 40 % of the surface water cannot meet the national standard for drinking source water in China (Feng et al. 2012). The conventional water treatment process including coagulation/flocculation, sand filtration and chlorination can only remove about 30 % of organic matters in the source water (Chu et al. 2012; Simpson 2008). However, more than 80 % of the waterworks in China are still using such a conventional process which may not be able to produce drinking water with the desired quality according to the tightened national water quality regulations (Dong et al. 2014; Zhao et al. 2015). Therefore, the process upgrading is urgently needed.

So far, many alternative techniques including advanced oxidation, nanofiltration, reverse osmosis and activated carbon have been explored for upgrading the existing water

✉ Z. Wang
wangzheng@njfu.edu.cn

1 School of Civil Engineering, Nanjing Forestry University, 159 Longpan Road, Nanjing 210037, China

2 Advanced Environmental Biotechnology Centre, Nanyang Environment and Water Research Institute, Nanyang Technological University, 1 Cleantech Loop, Singapore 637141, Singapore

3 School of Civil and Environmental Engineering, Nanyang Technological University, 50 Nanyang Avenue, Singapore 639798, Singapore

4 School of Chemical Engineering and Energy, Zhengzhou University, 100 Science Avenue, Zhengzhou 450001, China

treatment facility, but there are the questions regarding the cost-effectiveness, availability of space site, process sustainability, etc. (Benner et al. 2013; Dorival-Garcia et al. 2014; Safari et al. 2015). Recently, biological activated carbon (BAC) process coupled with ozonation has been seriously considered as an effective method for treating micropolluted drinking source water (Lautenschlager et al. 2014; Liao et al. 2013). It should be noted that this combined ozonation-activated carbon process has drawbacks of high capital and operating costs, large space requirement as well as issues associated with daily maintenance. These in turn suggest that such an advanced treatment process may not be suitable for many waterworks in China which are lack of financial support and space (Yang et al. 2010).

Biofiltration, a combination of physical filtration and biological degradation, has been developed for removing low-concentration pollutants (e.g., organic matters, ammonia, micropollutants, odor-causing compounds and disinfectant by-products) from source water during drinking water production (Purswani et al. 2014; Black and Berube 2014; Pharand et al. 2014). The successful key of biofiltration process is replacing quartz sand of conventional filter such as V-type filter to biological filter media and providing an excellent environment for the growth of biofilm (Zhang et al. 2014). Granular activated carbon (GAC) as one of the most widely used biological filter media has high sorption capacity to remove pollutants because of GAC's porous structure and high specific surface area (Yapsakli and Cecen 2010). But potential loss risk during backwashing process because of GAC's specific density much lighter compared with mineral filter media and its high cost restrict the all or part replacement of the quartz sand filter to achieve well biofiltration function (Kennedy et al. 2015).

Suitable adsorptive-type filter material with appropriate biofiltration properties should be developed and manufactured to replace quartz sand and improve the efficiency of biofiltration on treatment of micropolluted drinking source water. Attapulgite as one kind of abundant storage's clay mineral in China is widespread and cheap and has large internal high specific surface and good adsorption ability. In our previous study, attapulgite composite ceramsite (ACC) was initially applied in water treatment field and exhibited good performance characteristics (Wang et al. 2009).

In this research, pilot start-up and steady-state affecting factors of attapulgite composite ceramsite/quartz sand double-layer biofilter (ACC/QSDLBF) and quartz sand single-layer biofilter (QSSLBF) on micropolluted drinking source water treatment were studied. Removal efficiencies of organic matters, ammonia and turbidity in start-up phase from micropolluted drinking water using these two biofilters were assessed. In stable phase, head loss changes in the two biofilters were analyzed. The effect of filter layer depth and hydraulic loading toward organic matter removal rate in the two biofilters were discussed. The outcomes of this research have a realistic significance to design and practical application of ACC for new construction of waterworks, especially upgrading of existing waterworks treating micropolluted drinking source water.

Materials and methods

Preparation of ACC

Attapulgite composite ceramsites used in this pilot study were manufactured with attapulgite powder (100 mesh) as main raw material, adding 10 wt% of zeolite powder (100 mesh) and 10 wt% of kaolin powder (100 mesh). First, the three kinds of mineral material powder with above-mentioned proportion were mixed and stirred uniformly to obtain granular raw material. Second, the granular raw material was fed to disk granulator to obtain spherical semifinished attapulgite composite ceramsites (about 5 wt% of water was added in this process). Third, the semifinished ceramic particles were dried at 150 °C for 3 h to dewater. Fourth, put the dried ceramic particles in the furnace, and the internal temperature of furnace was increased in step of 5 °C/min to the desired temperature 800 °C, keeping for 2 h. Finally, the finished attapulgite composite ceramsites were cooled to ambient temperature naturally (Wang 2015).

Pilot devices and micropolluted source water

Schematic diagram of the pilot devices is shown in Fig. 1. The inner diameter of the filter column was 10 cm, and the height was 300 cm. Sampling tap, filter material sampling port and piezometric measurement pipe were arranged upon supporting layer (gravel) every 20 cm. The upper layer of ACC/QSDLBF was filled with 80-cm ACC ($d_{10} = 4.5 \pm 0.5$ mm, $K_{80} = 1.1$–1.2), and the lower layer was filled with 40 cm of height quartz sand ($d_{10} = 1.0 \pm 0.05$ mm, $K_{80} = 1.3$–1.4). Supporting layer (gravel) height was 20 cm with diameter of 8–12 mm. The quartz sand filter column was filled with thickness of 120-cm quartz sand, and the supporting layer (gravel) height was same as ACC/QSDLBF. Other device components consisted of an influent tank, a backwashing tank, flowmeters installed in the outflow pipeline of two filters, water distributors above the filters, controlling valves, long-handled filter head, air compressor supplying backwashing air and two centrifugal pumps for influent and backwashing water supply.

The feedwater was made up with polluted river water and overnight tap water at a volumetric ratio of 1:20 (Jing

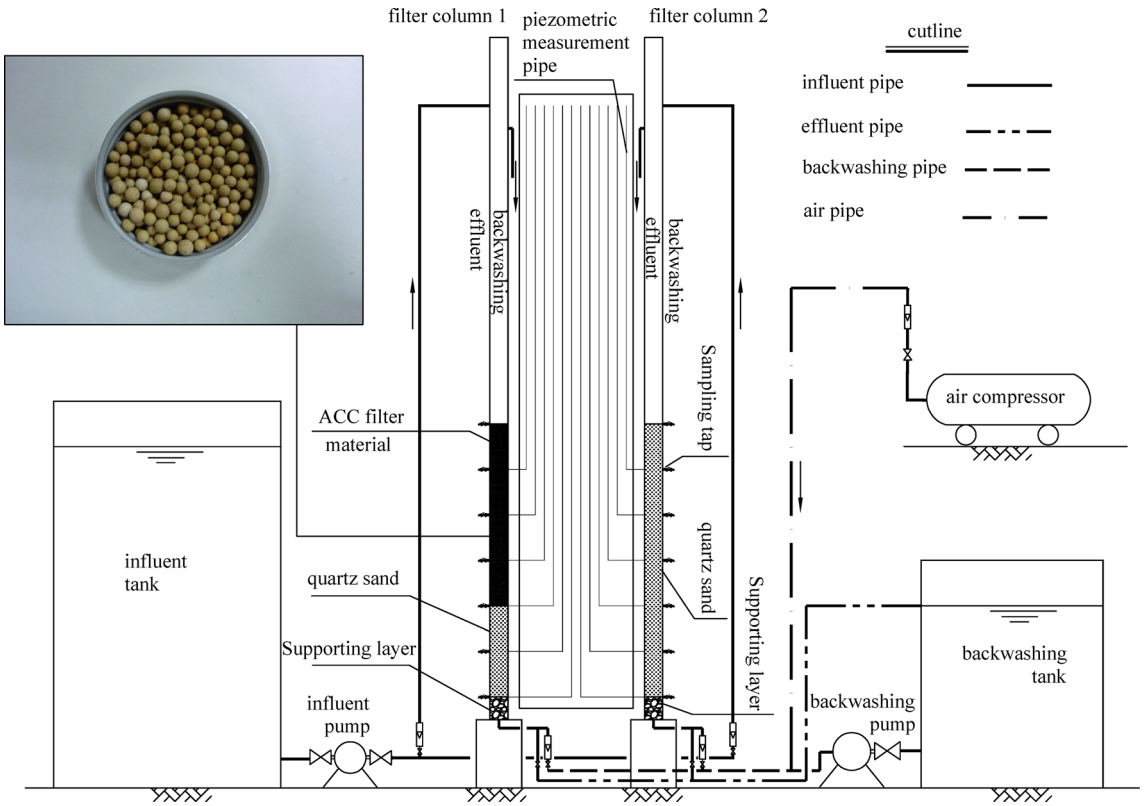

Fig. 1 Schematic diagram of the pilot system

et al. 2012). The characters of the micropolluted water source such as the temperature, dissolved oxygen content, turbidity, permanganate index (COD_{Mn}) and ammonia concentration during the pilot experiment were 19–25 °C, 3.23–7.52 mg/L, 0.523–3.19 NTU, 1.97–5.54 mg/L and 0.32–1.72 mg/L, respectively.

Start-up and operation of the biofilters

The two biofilters were operated in parallel with a down-flow velocity of 8 m/h, while the empty bed contact time (EBCT) was controlled at 9 min in the filter media. The effective water depth upon the filter layer was 120 cm. The treated water was discharged directly after biofiltration. When the water head loss reached 100 cm or the turbidity of finished water exceeded 0.5 NTU, backwashing was initiated. Backwashing water from the tank was treated effluent and only with low flow water rinse in start-up phase of two biofilters, normal joint air and water rinse, was used in operation phase with no expansion rate.

Analytical methods

The conventional indices of water quality, including COD_{Mn} and NH_4^+-N, were determined according to standard examination methods for drinking water (GB/5750-2006, China). Turbidity was measured with a turbidity instrument (2100N, Hach instrument, USA). A scanning electron microscope (Quanta 200, Fei Instrument, Holland) was used to obtain the characterization of the surface morphology and fundamental physical properties of the ACC. The intrusion data including pore surface area and the pore size distribution of the ACC were carried out by using a mercury porosimeter (Autopore 9500, Micromeritics Instrument, USA). The predominant elements of ACC were analyzed using an energy-dispersive X-ray spectrometer (EDX) (Inca, Oxford Instrument, England).

Results and discussion

Characterization of ACC

The scanning electron microscopic (SEM) images of ACC's surface and section under 4000 magnifications are shown in Fig. 2a, b. From these two figures, we can find that the ACC has coarse, irregular and porous surface, meanwhile a large number of well-developed uneven holes and cracks inside. In the adsorptive removal and biological filtration process, the ACC's surface and internal fully developed pores and cracks can provide space for

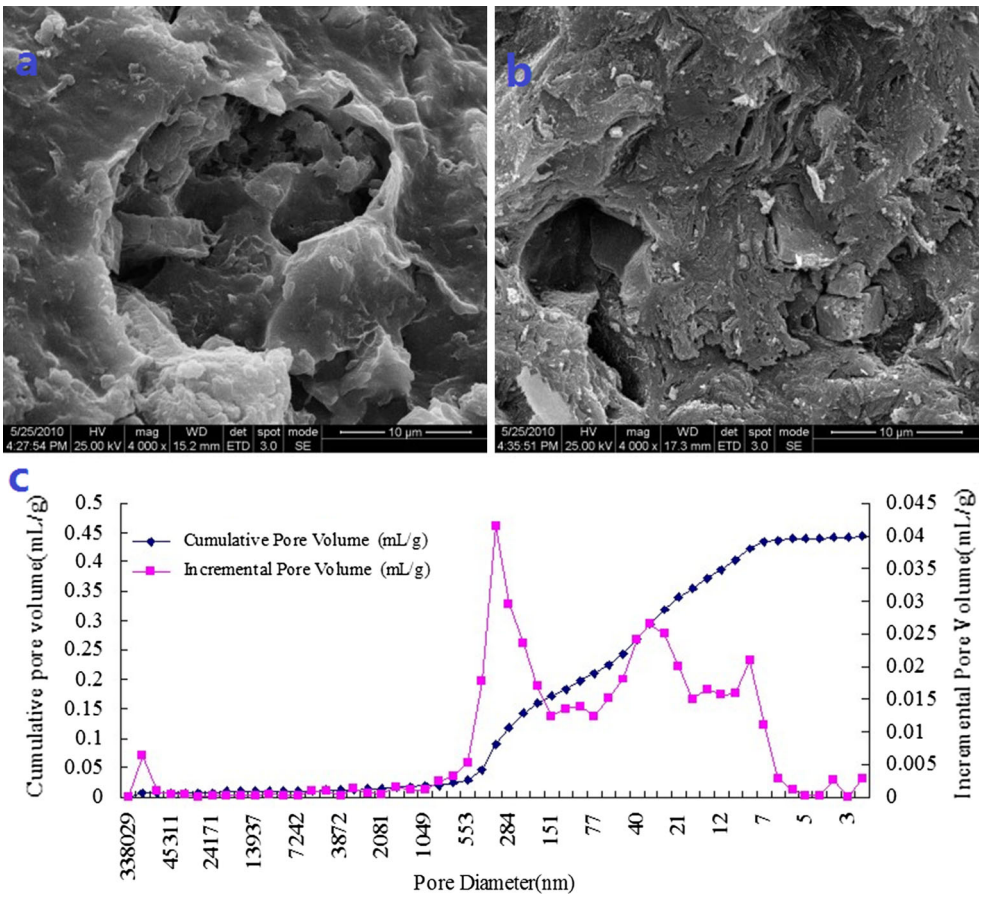

Fig. 2 Scanning electron microscopic (SEM) images of ACC's surface (**a**), section (**b**) under 4000 magnifications and the pore size distribution of ACC (**c**)

attachment of microorganisms, as well as providing exchange channel between the microbial cells and matrix, which will be conducive to metabolism of microorganisms and removal of pollutants from micropolluted drinking source water (Wu et al. 2015).

Porous structure parameters of ACC acquired by mercury porosimeter are total intrusion volume (V_{ti}) = 0.4442 mL/g, total pore area (A_t) = 57.905 m^2/g and average pore diameter ($4V/A$) (D_a) = 30.7 nm. The pore size of ACC ranged from 8 to 400 nm (Fig. 2c), indicating that the ACC has hybrid characteristics of mesoporous ($2\ nm < d < 50\ nm$) and macroporous ($d > 50$ nm) structure (Wang 2015). It should also be noted that the pore size range of ACC is much wider than that of GAC typically in the range of 0.7–2 nm (Gibert et al. 2013a, b). In general, almost all bacteria are larger than 200 nm in size; hence, they cannot penetrate into GAC micropores (Yapsakli and Cecen 2010). In fact, such a highly porous structure of ACC with reasonable pore size distribution favors adsorption of organic matters, while providing large surface area for microorganisms to adhere on (Schwartz et al. 2009).

The chemical elements of the ACC determined by energy-dispersive X-ray spectrometer (EDX) are shown in Table 1. It confirms that the main elements of the ACC are composed of oxygen, silicon, aluminum, iron, magnesium, calcium and titanium being similar to quartz sand. No heavy metals were detected in the ACC used in this study, suggesting that use of ACC as a biofilter material for drinking water production would be considered safe.

Organic matter removal in ACC/QSDLBF and QSSLBF during start-up phase

In this study, permanganate index (COD_{Mn}), rather than dissolved organic carbon (DOC), was chosen to indicate the removal efficiency of organic matters, because COD_{Mn} was the surrogate parameter of organic matter in drinking water in the latest national standard (GB5749-2006) of China (Han et al. 2013a, b). The COD_{Mn} removal efficiency of ACC/QSDLBF and QSSLBF is shown in Fig. 3. The early COD_{Mn} removal of ACC/QSDLBF can reach more than 30 %, mainly due to

Table 1 Elemental composition of ACC used in this study

Element	O	Si	Al	Mg	Fe	Ca	Ti
%	47.41	31.33	9.22	5.96	3.97	1.58	0.53

ACC's large specific surface area and reasonable pore size distribution which supplies a large number of adsorptive sites toward the organic matter, meanwhile interception of the filter layer removing a certain number of non-dissolved organic matters in raw water (Gibert et al. 2013a, b). With the continuous influent and gradual saturation of ACC's adsorptive ability, the removal of COD_{Mn} declined and appeared to no effect at day 6 and day 10. During this stage, the ACC was exposed to the microbial community present in the water, which contributed to a rapid initial colonization. Despite the apparent saturation of ACC's adsorptive sites, the removal began to increase at day 11, with approximately 20–25 % steady COD_{Mn} removal from day 22 onward. This stable removal was due to biodegradation by microorganisms that colonizing on the ACC comparable to previous study (Velten et al. 2011). After this stage, the filter operated in steady state, in which almost all removal of organic matter occurs via bio-oxidation, and adsorption by the filter material was insignificant. Thus, bio-oxidation plays a dominant role in the removal of dissolved organic carbon in the biofilter (Zhang et al. 2015). Interception of ACC/QSDLBF plays another important role in the non-soluble organic substance removal.

The COD_{Mn} removal of QSSLBF was relatively stable, with an average removal rate of about 6 % mainly depending on physical interception of non-soluble organics through quartz sand filter. The biodegradation by heterotrophic bacteria of quartz sand was much weaker compared with ACC due to smooth and compact surface being difficult for biofilm attachment and growth on it.

Ammonia removal in ACC/QSDLBF and QSSLBF during start-up phase

Ammonia present in raw water is mostly in the form of ammonium (NH_4^+-N), which increases the chlorine demand and acts as a precursor of trichloramine under some conditions, thereby yielding an undesirable odor and taste to potable water (Niu et al. 2013). Indeed, the drinking water national standard (GB5749-2006) of China requests the ammonia concentration in tap water to a relatively low level (<0.5 mg/L). The NH_4^+-N removal efficiency of ACC/QSDLBF and QSSLBF is shown in Fig. 4. As depicted in Fig. 4, NH_4^+-N removal rate of ACC/QSDLBF was about 35 % because of adsorptive function of ACC. Subsequent removal of NH_4^+-N began gradually decreased, mainly due to the saturation of ACC's adsorption ability. NH_4^+-N removal rate on day 7 was down to 15 %. From day 12, NH_4^+-N removal rate gradually increased, indicating that nitrification bacteria have gradually attached to the ACC. It was well known that the carbon sources in drinking water are usually insufficient for the conversion of NH_4^+-N to nitrogen gas by the conventional nitrification–denitrification process. Therefore, NH_4^+-N is believed to be converted to nitrate by nitrification with the consumption of DO (Lu et al. 2015; Cai et al. 2014). The increase in biomass was due to the favorable conditions for heterotrophic bacteria due to the organic carbon provided for their synthesis in start-up stage, which consequently increased the removal of NH_4^+-N and COD_{Mn} (Abu Hasan et al. 2014). The influent NH_4^+-N concentration on day 23 was of about 0.8 mg/L, and the NH_4^+-N removal efficiency reached 83.8 %,

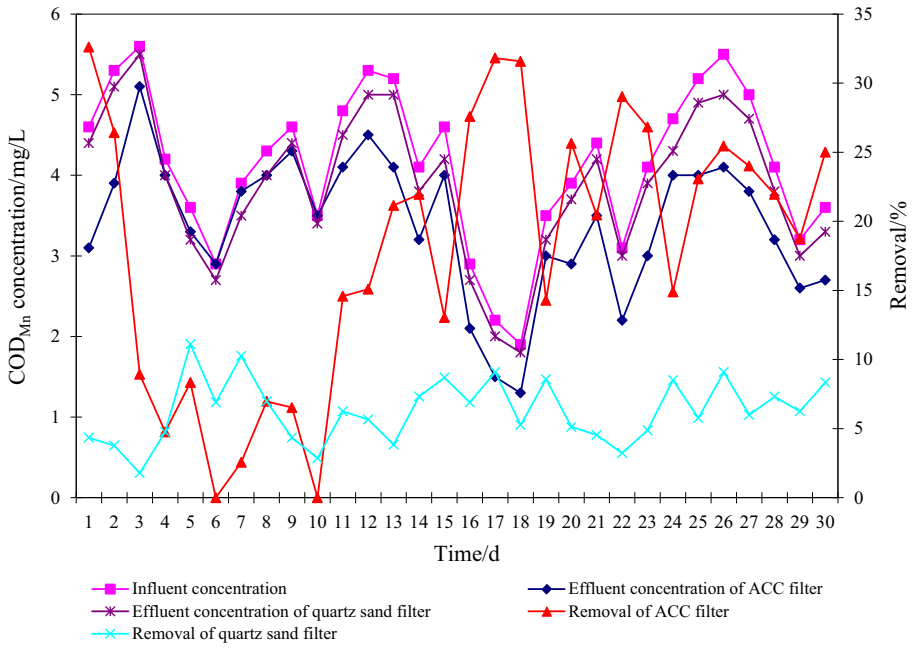

Fig. 3 COD_{Mn} removal in ACC/QSDLBF and QSSLBF during start-up phase

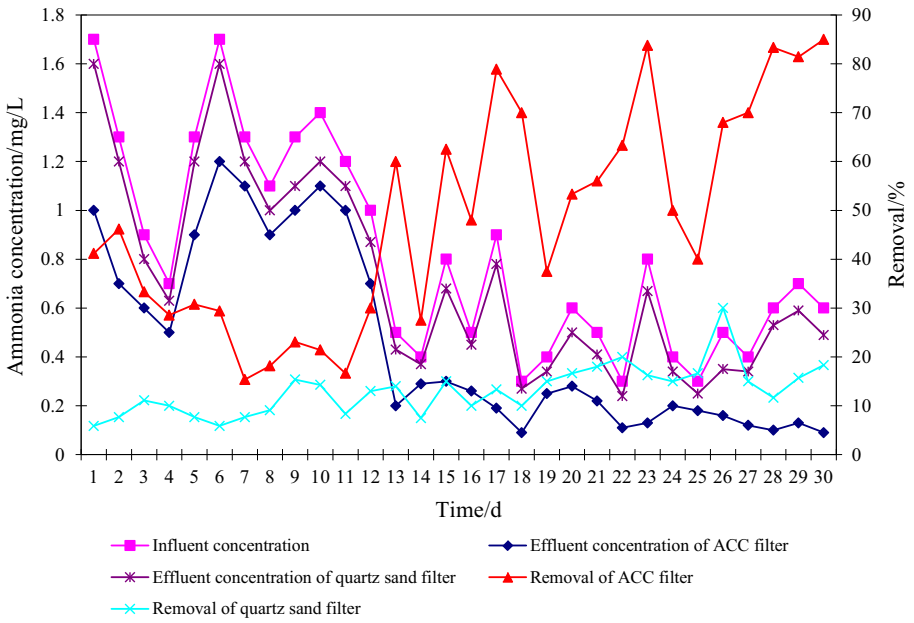

Fig. 4 NH_4^+-N removal in ACC/QSDLBF and QSSLBF during start-up phase

indicating the stable biological nitrification for ACC/QSDLBF system. van den Akker et al. (2008) observed that characteristic removal of influent ammonia-N happened within 14 days and coincided with production of nitrite and nitrate, which was similar to the results of our study. Cai et al. (2015) found that biofilter inoculated with nitrifying sludge needed about 9 days to obtain a lower effluent ammonia concentration. The mature time of nitrobacteria in biofilm inoculated with nitrifying sludge was faster than our natural start-up.

The NH_4^+-N removal efficiency of QSSLBF has the similar trend as organic matter with 13 % removal rate in this stage. Nitrification is a two-step biological process conducted by autotrophic bacteria and archaea. First, ammonia-oxidizing bacteria (AOB) or archaea (AOA) oxidize ammonium to nitrite, which is then oxidized to nitrate by nitrite-oxidizing bacteria (NOB) (Lee et al. 2014). Due to its poor microbial adhered performance for autotrophic bacteria and archaea, the NH_4^+-N average removal of QSSLBF was a quarter of the ACC/QSDLBF after formation of mature biofilm.

Turbidity removal in ACC/QSDLBF and QSSLBF during start-up phase

Turbidity not only is an important sensory parameter in the water industry, but also serves as a carrier for nutrients and pathogens. Moreover, turbidity is applied in assessing the effectiveness of the filtration process and the quality of drinking water (Simate 2015). As shown in Fig. 5, the two filtration columns both had relatively high turbidity removal rate. When influent turbidity was between 0.78 and 2.9 NTU, effluent turbidity of ACC/QSDLBF was 0.09–0.42 NTU with average removal rate 86.7 % and QSSLBF was 0.08–0.4 NTU with average removal rate 89.5 %. Average removal rate of ACC/QSDLBF was lower 2.8 % than QSSLBF due to greater porosity of ACC filtration layer of 80 cm thickness. In the ACC itself, the turbidity was principally removed through two processes. First, physical straining was realized by trapping the particulate matter between the grains of ACC. Second, the particulates in water attached themselves to oligotrophs biofilm on ACC or to previously retained particles in biofiltration phase in ACC/QSDLBF. The turbidity removal rate of the two filtration columns improved at a certain degree in the last stage of start-up and stable-stage mainly due to increased biological adsorption of active flocculent filtration layer attached on the ACC and quartz sand (Simate 2015).

Development of head loss in ACC/QSDLBF and QSSLBF during steady-state period

In steady operation phase, the head loss growth of ACC/QSDLBF and QSSLBF in a complete filtration cycle (with effluent turbidity exceeding 0.5 NTU as stopping filtration and backwashing sign) was investigated through piezometric measurement pipe, and the result is shown in Fig. 6. As shown in Fig. 6, the initial head loss of ACC/QSDLBF and QSSLBF was 12 and 20 cm. From filtration beginning to effluent turbidity exceeding 0.5 NTU, the head loss of QSSLBF increased 87 cm and reached 107 cm after 32 h. At the same period, the head loss of ACC/QSDLBF increased 56 cm to 68 cm. The complete filtration cycle of

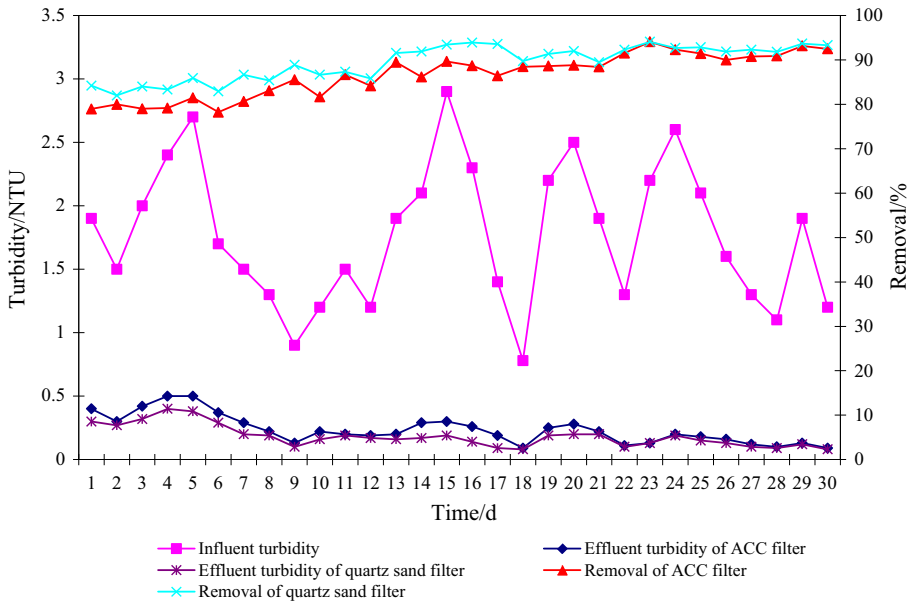

Fig. 5 Turbidity removal in ACC/QSDLBF and QSSLBF during start-up phase

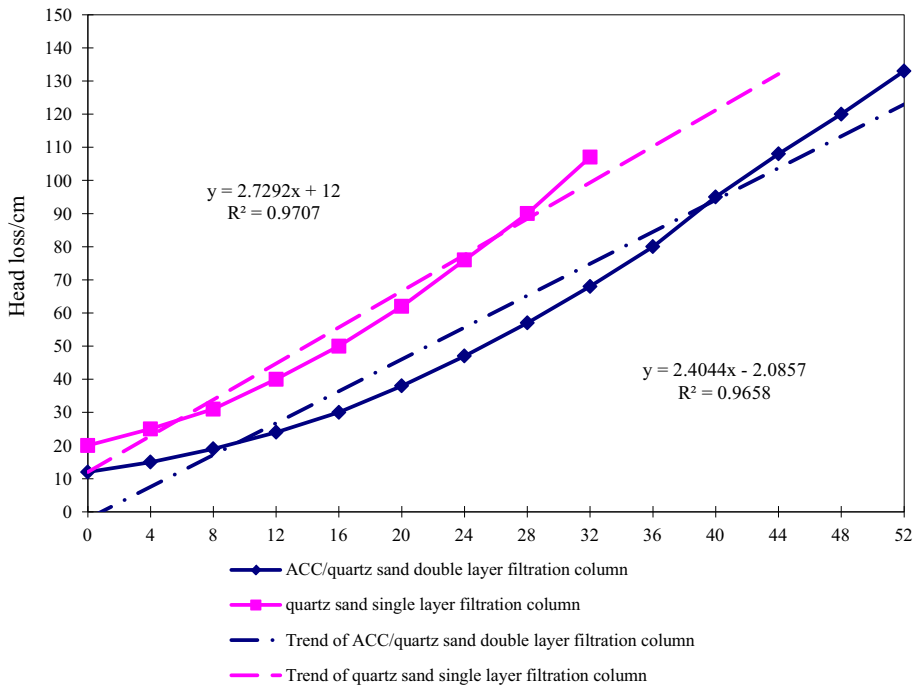

Fig. 6 Evaluation of head loss in ACC/QSDLBF and QSSLBF during steady state

ACC/QSDLBF can reach 52 h, illustrating higher interception capability toward QSSLBF, and the total head loss can achieve 133 cm with increase of 121 cm. The head loss growth trend line's slope of ACC/QSDLBF (2.4044) is lower than that (2.7292) of QSSLBF, which indicated that the average growth rate of head loss in ACC/QSDLBF is slower than head loss growth rate in QSSLBF. The better hydraulic condition of ACC filtration layer owing to larger size and higher sphericity compared with quartz sand is conducive to reduce the initial and operational head loss and extend the filtration cycle. Relatively low head loss growth and long filtration run enabled high mass capacity (Jez-Walkowiak et al. 2015). The average speed of head loss growth during the later 28 h in ACC/QSDLBF (86 cm) was significantly faster than that (35 cm) of the first 24 h. The detached retained particles and biofilm due to increased shearing forces resulting from filter clogging can enter the deeper filter layer's fissure of ACC/QSDLBF and lead rapid growth of head loss during the later biofiltration phase (Gholikandi et al. 2012).

Effect of depth in ACC/QSDLBF and QSSLBF on COD_{Mn} removal during steady-state period

The effect of depth in ACC/QSDLBF and QSSLBF on COD_{Mn} removal during steady-state period was taken to analyze stratified effluent, and the results are enumerated in Table 2. The total removal rate of COD_{Mn} in ACC/QSDLBF and QSSLBF was 20.93 and 6.89 %, respectively. The 75 % of total COD_{Mn} removal in ACC/QSDLBF accomplished in the first 40-cm-thickness ACC filter layer, and 90 % of total COD_{Mn} removal achieved with depth being 60 cm. At the bottom of quartz sand filtration layer in ACC/QSDLBF, little COD_{Mn} removal was observed. The biomass accumulated rapidly in the upper layer of ACC/QSDLBF, and biodegradation removal occurred at the top of the biofilter, whereas the lower growth rate at the bottom of ACC/QSDLBF was ascribed to a decreasing availability of organic nutrients downward through the filter (Xiang et al. 2013). Considering that organic matter removal in the biofilter is roughly proportional to existing biomass, the result was along the expected lines (Kalkan et al. 2011). In study of Liao et al. (2013), DOC and AOC were mainly removed in the first-stage BAC filter, especially in the top 20-cm GAC layer. Therefore, DOC and AOC removal differentiated in the biofiltration system. Yapsakli and Cecen (2010) made a similar comparison in drinking water biofilters and showed that 42 % of the DOC was biodegraded in the first 25 cm of BAC column and another 5 % in the lower part of the column despite the existence of sufficient bacteria. In our research, ACC's size and sphericity were much larger than GAC. Relatively more proportion of suspended solids and organic matters could enter into deeper ACC filter layer and decline of biomass density in ACC filtration layer was less than in GAC filtration layer, and therefore 90 % of total COD_{Mn} removal was achieved in the top 60-cm ACC filtration layer.

Most of the COD_{Mn} removal in QSSLBF occurred in the first 40-cm-thickness quartz sand layer, and the surface 20-cm quartz sand accomplished 67.69 % total COD_{Mn} removal. Compared with ACC/QSDLBF and BAC, the COD_{Mn} removal of QSSLBF was largely dependent on the interception of insoluble organic matters, and the dissolved organic matter removal was low due to weak biodegradation capacity with respect to low existing biomass (Kalkan et al. 2011).

Table 2 COD_{Mn} removal of different depth in ACC/QSDLBF and QSSLBF during steady state

Depth (cm)	Removal in ACC/QSDLBF (%)	Removal in QSSLBF (%)
0	0	0
20	10.47	4.65
40	15.12	6.87
60	17.44	6.92
80	19.77	6.93
100	20.91	6.91
120	20.93	6.89

Effect of hydraulic loading in ACC/QSDLBF and QSSLBF on COD_{Mn} removal during steady-state period

The effect of hydraulic loading in ACC/QSDLBF and QSSLBF on COD_{Mn} removal during steady-state period was taken to analyze final effluent under different hydraulic loadings, and the results are enumerated in Table 3. It was apparent that it greatly decreased the removal of COD_{Mn} from 35.89 to 13.16 % in ACC/QSDLBF and 13.16 to 3.95 % in QSSLBF when increasing hydraulic loading from 2 to 16 m/h, but there was little change (21.25–18.29 %) in ACC/QSDLBF for removal rate of COD_{Mn} when hydraulic loading increased from 6 to 12 m/h and little change (5.26–4.76 %) in QSSLBF when hydraulic loading changes from 10 to 14 m/h. Diffusion rate of organic matters in water toward biofilm and biodegradation time inside biofilm directly determines the removal of organic matters. The high hydraulic loading decreased the diffusion rate and biodegradation time of organic matters in biofilm, meanwhile increased shear forces being a major hindrance for biofilm development and interception of pollutants through filter media (Yapsakli and Cecen 2010).

The capacity of a biofiltration water treatment system could be greatly affected by the hydraulic loading, which directly relates to empty bed contact time (EBCT) of the filter. High hydraulic loading cannot guarantee that impurities were completely degraded, while low hydraulic loading would increase the construction cost of the system. Therefore, hydraulic loading should be optimized by considering the cost and the system performance (Han et al. 2013a, b). In order to evaluate the optimized hydraulic loading or EBCT of filter meeting final effluent limits, we first put forward a concept of efficient EBCT (EEBCT) to our knowledge. EEBCT was calculated through COD_{Mn} or main objective substance removal rate (%) dividing EBCT (min) in filter, and the greater of the ratio indicating more economic of filter's scale under permitted final effluent limits. The calculated conclusions of EEBCT in ACC/QSDLBF and QSSLBF are summarized in Table 3. When EBCT is 36 min and hydraulic loading is 2 m/h, EEBCT in ACC/QSDLBF and QSSLBF were 1.0 and 0.36, indicating the worst economy of the two filters at this operational condition, and the economy of ACC/QSDLBF was much higher than that of QSSLBF. The highest EEBCT in ACC/

Table 3 COD_{Mn} removal under different EBCT and removal/EBCT in the two biofilters during steady state

EBCT (min)	Hydraulic loading (m/h)	Removal in ACC/QSDLBF (%)	Removal in QSSLBF (%)	Removal/EBCT in ACC/QSDLBF	Removal/EBCT in QSSLBF
36	2	35.89	12.82	1.00	0.36
18	4	26.83	9.76	1.49	0.54
12	6	21.25	7.50	1.77	0.63
9	8	20.93	6.97	2.32	0.78
7.2	10	19.74	5.26	2.74	0.73
6	12	18.29	4.88	3.05	0.81
5.1	14	14.29	4.76	2.80	0.93
4.5	16	13.16	3.95	2.92	0.88

QSDLBF was 3.05 with 18.29 % COD_{Mn} removal when hydraulic loading is 12 m/h (EBCT = 6 min), and the highest EEBCT in QSSLBF was 0.93 with 4.76 % COD_{Mn} removal when hydraulic loading is 14 m/h (EBCT = 5.1 min). The COD_{Mn} removal in ACC/QSDLBF under hydraulic loading being 8 m/h (EBCT = 9 min) was similar to hydraulic loading being 12 m/h (EBCT = 6 min). The difference EEBCT of these two hydraulic loadings was 0.73, and the relatively large difference indicated that hydraulic loading being 12 m/h is more economic than 8 m/h in ACC/QSDLBF.

Conclusion

This study showed that the ACC has suitable pore size distribution conducive to biofiltration and is safe being used in drinking water treatment scale. Turbidity removal efficiency of ACC/QSDLBF was a little lower than QSSLBF, but organic matters and ammonia removal efficiencies of ACC/QSDLBF were much higher than QSSLBF. In stable state, head loss growth of ACC/QSDLBF was lower than QSSLBF and the complete filtration cycle of ACC/QSDLBF was much longer than QSSLBF. The most of total COD_{Mn} removal rate in ACC/QSDLBF was achieved in ACC filtration layer. The removal of COD_{Mn} greatly decreased in ACC/QSDLBF when hydraulic loading increases from 2 to 16 m/h. The optimized hydraulic loading was 12 m/h based on EEBCT analysis in ACC/QSDLBF. These conclusions contributed to practical application of ACC for new waterworks construction and upgrading of existing waterworks of micropolluted drinking source water.

Acknowledgments The authors express their sincere gratitude to the Housing and Urban and Rural Construction Technology Program of the Ministry of Science and Project (2011-K7-2), the project of Jiangsu government scholarship for study abroad (2012196) and a project funded by the Priority Academic Program Development of the Jiangsu Higher Education Institutions (PAPD) for financial support.

References

Abu Hasan H, Abdullah SRS, Kamarudin SK, Kofli NT, Anuar N (2014) Kinetic evaluation of simultaneous COD, ammonia and manganese removal from drinking water using a biological aerated filter system. Sep Purif Technol 130:56–64

Benner J, Helbling DE, Kohler H-PE, Wittebol J, Kaiser E, Prasse C, Ternes TA, Albers CN, Aamand J, Horemans B, Springael D, Walravens E, Boon N (2013) Is biological treatment a viable alternative for micropollutant removal in drinking water treatment processes? Water Res 47(16):5955–5976

Black KE, Berube PR (2014) Rate and extent NOM removal during oxidation and biofiltration. Water Res 52:40–50

Cai YA, Li D, Liang YH, Zeng HP, Zhang J (2014) Autotrophic nitrogen removal process in a potable water treatment biofilter that simultaneously removes Mn and NH_4^+-N. Bioresour Technol 172:226–231

Cai YN, Li D, Liang YW, Luo YH, Zeng HP, Zhang J (2015) Effective start-up biofiltration method for Fe, Mn, and ammonia removal and bacterial community analysis. Bioresour Technol 176:149–155

Chu HQ, Dong BZ, Zhang YL, Zhou XF, Yu ZX (2012) Pollutant removal mechanisms in a bio-diatomite dynamic membrane reactor for micro-polluted surface water purification. Desalination 293:38–45

Dong LH, Liu WJ, Jiang RF, Wang ZS (2014) Physicochemical and porosity characteristics of thermally regenerated activated carbon polluted with biological activated carbon process. Bioresour Technol 171:260–264

Dorival-Garcia N, Zafra-Gomez A, Oliver-Rodriguez B, Navalon A, Gonzalez-Lopez J, Vilchez JL (2014) Effect of the injection of pure oxygen into a membrane bioreactor on the elimination of bisphenol A. Int J Environ Sci Technol 11(1):9–20

Feng S, Xie SG, Zhang XJ, Yang ZY, Ding W, Liao XB, Liu YY, Chen C (2012) Ammonium removal pathways and microbial community in GAC-sand dual media filter in drinking water treatment. J Environ Sci China 24(9):1587–1593

Gholikandi GB, Noorisepehr M, Dehghanifard E, Koolivand A, Dehnavi A, Moalej S (2012) Application of modified qualitative index for surveillance of water-filtration process in turbidity removal by different media. Int J Environ Sci Technol 9(4):691–700

Gibert O, Lefevre B, Fernandez M, Bernat X, Paraira M, Pons M (2013a) Fractionation and removal of dissolved organic carbon in a full-scale granular activated carbon filter used for drinking water production. Water Res 47(8):2821–2829

Gibert O, Lefevre B, Fernandez M, Paraira M, Calderer M, Martinez-Llado X (2013b) Characterising biofilm development on

granular activated carbon used for drinking water production. Water Res 47(3):1101–1110

Han LN, Liu WJ, Chen M, Zhang ML, Liu SM, Sun RL, Fei XQ (2013a) Comparison of NOM removal and microbial properties in up-flow/down-flow BAC filter. Water Res 47(14):4861–4868

Han M, Zhao ZW, Gao W, Cui FY (2013b) Study on the factors affecting simultaneous removal of ammonia and manganese by pilot-scale biological aerated filter (BAF) for drinking water pretreatment. Bioresour Technol 145:17–24

Jez-Walkowiak J, Dymaczewski Z, Weber L (2015) Iron and manganese removal from groundwater by filtration through a chalcedonite bed. J Water Supply Res Technol 64(1):19–34

Jing ZQ, Li YY, Cao SW, Liu YY (2012) Performance of double-layer biofilter packed with coal fly ash ceramic granules in treating highly polluted river water. Bioresour Technol 120:212–217

Kalkan C, Yapsakli K, Mertoglu B, Tufan D, Saatci A (2011) Evaluation of biological activated carbon (BAC) process in wastewater treatment secondary effluent for reclamation purposes. Desalination 265(1–3):266–273

Kennedy AM, Reinert AM, Knappe DRU, Ferrer I, Summers RS (2015) Full-and pilot-scale GAC adsorption of organic micropollutants. Water Res 68:238–248

Lautenschlager K, Hwang C, Ling FQ, Liu WT, Boon N, Koster O, Egli T, Hammes F (2014) Abundance and composition of indigenous bacterial communities in a multi-step biofiltration-based drinking water treatment plant. Water Res 62:40–52

Lee CO, Boe-Hansen R, Musovic S, Smets B, Albrechtsen HJ, Binning P (2014) Effects of dynamic operating conditions on nitrification in biological rapid sand filters for drinking water treatment. Water Res 64:226–236

Li YP, Tang CY, Yu ZB, Acharya K (2014) Correlations between algae and water quality: factors driving eutrophication in Lake Taihu, China. Int J Environ Sci Technol 11(1):169–182

Liao XB, Chen C, Wang Z, Wan R, Chang CH, Zhang XJ, Xie SG (2013) Changes of biomass and bacterial communities in biological activated carbon filters for drinking water treatment. Process Biochem 48(2):312–316

Lu CQ, Li S, Gong S, Yuan SJ, Yu X (2015) Mixing regime as a key factor to determine DON formation in drinking water biological treatment. Chemosphere 139:638–643

Niu J, Kasuga I, Kurisu F, Furumai H, Shigeeda T (2013) Evaluation of autotrophic growth of ammonia-oxidizers associated with granular activated carbon used for drinking water purification by DNA-stable isotope probing. Water Res 47(19):7053–7065

Pharand L, Van Dyke MI, Anderson WB, Huck PM (2014) Assessment of biomass in drinking water biofilters by adenosine triphosphate. J Am Water Works Assoc 106(10):63–64

Purswani J, Silva-Castro GA, Guisado IM, Gonzalez-Lopez J, Pozo C (2014) Biological and chemical analyses of a laboratory-scale biofilter for oxygenate bioremediation in simulated groundwater. Int J Environ Sci Technol 11(6):1517–1526

Safari GH, Hoseini M, Seyedsalehi M, Kamani H, Jaafari J, Mahvi AH (2015) Photocatalytic degradation of tetracycline using nanosized titanium dioxide in aqueous solution. Int J Environ Sci Technol 12(2):603–616

Schwartz T, Jungfer C, Heissler S, Friedrich F, Faubel W, Obst U (2009) Combined use of molecular biology taxonomy, Raman spectrometry, and ESEM imaging to study natural biofilms grown on filter materials at waterworks. Chemosphere 77(2):249–257

Simate GS (2015) The treatment of brewery wastewater for reuse by integration of coagulation/flocculation and sedimentation with carbon nanotubes 'sandwiched' in a granular filter bed. J Ind Eng Chem 21:1277–1285

Simpson DR (2008) Biofilm processes in biologically active carbon water purification. Water Res 42(12):2839–2848

van den Akker B, Holmes M, Cromar N, Fallowfield H (2008) Application of high rate nitrifying trickling filters for potable water treatment. Water Res 42(17):4514–4524

Velten S, Boller M, Koster O, Helbing J, Weilenmann HU, Hammes F (2011) Development of biomass in a drinking water granular active carbon (GAC) filter. Water Res 45(19):6347–6354

Wang Z (2015) Efficient adsorption of dibutyl phthalate from aqueous solution by activated carbon developed from phoenix leaves. Int J Environ Sci Technol 12(6):1923–1932

Wang Z, Jing ZQ, Cheng LL, Shen W, Kong Y (2009) Adsorption of Cr(VI) by attapulgite–zeolite composite ceramsite from aqueous solution. Res J Chem Environ 13(4):13–17

Wu SQ, Qi YF, Yue QY, Gao BY, Gao Y, Fan CZ, He SB (2015) Preparation of ceramic filler from reusing sewage sludge and application in biological aerated filter for soy protein secondary wastewater treatment. J Hazard Mater 283:608–616

Xiang H, Lu XW, Yin LH, Yang F, Zhu GC, Liu WP (2013) Microbial community characterization, activity analysis and purifying efficiency in a biofilter process. J Environ Sci China 25(4):677–687

Yang JS, Yuan DX, Weng TP (2010) Pilot study of drinking water treatment with GAC, O_3/BAC and membrane processes in Kinmen Island, Taiwan. Desalination 263(1–3):271–278

Yapsakli K, Cecen F (2010) Effect of type of granular activated carbon on DOC biodegradation in biological activated carbon filters. Process Biochem 45(3):355–362

Zhang SF, Wang YY, He WT, Wu M, Xing MY, Yang J, Gao NY, Yin DQ (2013a) Responses of biofilm characteristics to variations in temperature and NH_4^+-N loading in a moving-bed biofilm reactor treating micro-polluted raw water. Bioresour Technol 131:365–373

Zhang YY, Hunt HK, Hu ZQ (2013b) Application of bacteriophages to selectively remove *Pseudomonas aeruginosa* in water and wastewater filtration systems. Water Res 47(13):4507–4518

Zhang SF, Wang YY, He WT, Wu M, Xing MY, Yang J, Gao NY, Pan ML (2014) Impacts of temperature and nitrifying community on nitrification kinetics in a moving-bed biofilm reactor treating polluted raw water. Chem Eng J 236:242–250

Zhang HN, Zhang KF, Jin HX, Gu L, Yu X (2015) Variations in dissolved organic nitrogen concentration in biofilters with different media during drinking water treatment. Chemosphere 139:652–658

Zhao F, Yin J, Zhang XX, Chen Y, Zhang Y, Wu B, Li M (2015) Reduction in health risk induced by semi-volatile organic compounds and metals in a drinking water treatment plant. Int J Environ Sci Technol 12(2):527–536